

# Electrochemical Preparation of Free-Standing Carbon-Nanotube/Sn Composite Paper

Masahiro Shimizu<sup>a,b,\*</sup>, Shunya Shimizu<sup>a</sup>, Arinobu Katada<sup>c</sup>,  
Mitsugu Uejima<sup>c</sup>, and Susumu Arai<sup>a,b,\*</sup>

<sup>a</sup> Department of Materials Chemistry, Faculty of Engineering, Shinshu University  
4-17-1 Wakasato, Nagano, 380-8553, Japan

<sup>b</sup> Institute of Carbon Science and Technology, Faculty of Engineering, Shinshu University  
4-17-1 Wakasato, Nagano, 380-8553, Japan

<sup>c</sup> Research & Development Center, Zeon Corporation,  
1-2-1 Yako, Kawasaki, Kanagawa, 210-9507, Japan

\*Corresponding Author E-mail Address [shimizu@shinshu-u.ac.jp](mailto:shimizu@shinshu-u.ac.jp), [araisun@shinshu-u.ac.jp](mailto:araisun@shinshu-u.ac.jp)

## Abstract

Toward achieving Li-ion batteries with high energy density, SWCNT/Sn composite paper was electrochemically prepared and the addition effect of formaldehyde (HCHO) and polyethylene glycol (PEG) on Sn electrodeposition morphology was studied. PEG improved the wettability of electroplating bath to enable inhomogeneous Sn embeddedness inside SWCNT paper, and HCHO delivered more nuclear growth. The synergetic effect resulted in a composite paper in which Sn particles with several-hundred nanometer order were distributed. Compared with a commercially-available Cu foil (18  $\mu\text{m}$ -thickness) with 32 mg at 2  $\text{cm}^2$  ( $\varphi$  16 mm), the weight of the SWCNT paper (5 mg) is one sixth of that of the Cu foil. The dramatic reduction of the component greatly contributes to the increase in energy density of batteries.

## Keywords:

Electrodeposition, Carbon nanotube, Sn, Negative electrode, Rechargeable battery

## 1. Introduction

Free-standing and flexible carbon nanotube (CNT) papers with porosity, aggregate of CNT bundles, have attracted much attention as a support matrix of catalyst and electrode materials in the energy scientific field.<sup>1,2</sup> For instance, composite papers in which Au and Pt are deposited inside functions as the cathode catalyst of glucose oxidation, and of oxygen reduction reaction for polymer electrolyte fuel cell.<sup>3</sup> In case of introducing Li storage substances (*e.g.*, the group 14 elements: graphite, Si, Sn and Sb), the resulting CNT composites can be a negative electrode for rechargeable batteries.<sup>4</sup> The motivation for the development of these energy-related materials is originated from high electrical conductivity and high chemical stability as well as high specific surface area of CNTs.<sup>5</sup> As for the latter, Sn is a promising active material due to its high gravimetric and volumetric capacities of 990 mA h g<sup>-1</sup> and 7313 mA h cm<sup>-3</sup> (Li<sub>4.4</sub>Sn) based on alloying/dealloying reactions with Li, and the capacities are much larger than those of currently-used graphite (372 mA h g<sup>-1</sup>, 883 mA h cm<sup>-3</sup>).<sup>6</sup> On the other hand, CNT paper is composed only of carbon, and the paper is ultra-lightweight compared with a commercially-used Cu substrate. Therefore, the use of CNT papers as a current collector should dramatically contribute to the achievement of miniaturization for electronics and wearable devices. However, the several research examples are limited to followings: (i) simple suction filtration of CNT-dispersed solution together with active material.<sup>1</sup> (ii) suction filtration of CNT which is coated with active material by impregnation, sputtering, and electroless deposition.<sup>7</sup> The method (i) causes inhomogeneous distribution (localization) of active material inside the composite electrodes. This is because of the difference in weight or density between CNT and the active materials, (*i.e.* CNT: 1.3–2.0 g cm<sup>-3</sup>, Sn: 7.3 g cm<sup>-3</sup>),<sup>3</sup> as shown in Figure S1. It is responsible for poor performance in catalyst and battery electrode. In contrast, our strategy is to introduce Sn inside CNT paper by electroplating technique. In the present study, we report the electrochemical preparation of CNT/Sn composite, and discuss the effect of additive in electroplating bath on Sn deposition behavior on CNT paper.

## 2. Experimental details

Single-walled CNT (SWCNT; Zeon Corp.)<sup>8</sup> synthesized by water-assisted chemical vapor deposition was added to deionized water and dispersed using sodium dodecylbenzenesulfonate

(SDBS). The content ratio of SWCNT was 0.2 wt.%, and the concentration of SDBS was  $3.0 \times 10^{-4}$  M. For the disintegration of SWCNT bundles formed by the strong van der Waals interaction, a wet-type jet mill (mechanical atomization) was applied to the suspension. The suspension (50 g) was then ultrasonically agitated and filtered using a membrane filter (Millipore) with a pore size of 0.1  $\mu\text{m}$ . The resulting agglomerate was washed by distilled water and dried at 80 °C for 12 h under vacuum to obtain a free-standing SWCNT paper with a 40- $\mu\text{m}$  thickness. The paper with an opening space area of  $2 \times 2 \text{ cm}^2$  as the cathode was placed at the center of an electrochemical cell, and was immersed in aqueous solutions consisted of 0.5 M  $\text{SnCl}_2$  + 1.25 M  $\text{K}_4\text{P}_2\text{O}_7$  + 5 mM formaldehyde (HCHO) + 2 mM polyethylene glycol (PEG, molecular weight: 600) for 30 min in advance. After setting up two Sn plates as the anode at either end of the cell, electrodeposition was conducted under a current density of  $1 \text{ mA cm}^{-2}$  ( $0.1 \text{ A dm}^{-2}$ ) at 25 °C without stirring. The charge amount was set to  $24 \text{ C cm}^{-2}$ .

### 3. Results and discussion

After treatment of a wet-type jet mill, SWCNT bundles were successfully disintegrated, as shown in high-resolution transmission electron microscope images (Figure 1). In the resulting SWCNT paper, we can observe pore structure with 80 nm or less on the surface. To obtain a SWCNT/Sn composite in which Sn is homogeneously distributed, the electrodeposition was conducted from both sides of the SWCNT paper. In Raman spectra of SWCNT papers (Figure 2), there is no significant change in D/G intensity ratio before and after the electrodeposition (Figure S2). The deposit was confirmed to be only  $\beta$ -Sn (ICSD: 00-004-0673). Interestingly, we cannot recognize Sn deposit when plating from one side.

In spite of the presence or absence of HCHO, no Sn particle was observed in interior portion of the SWCNT paper, and electrodeposition proceeded on only the SWCNT surface to form significantly large Sn particles of 10  $\mu\text{m}$  or more (Figure 3). In contrast, the use of PEG-600 led to homogeneous embeddedness of Sn in the form of particle with several-hundred nanometer order. We performed contact angle measurements by sessile drop method<sup>9</sup> to intuitively understand an indicator of wettability of electrolyte solution (Figure 4a). The contact angle of the additive-free electrolyte solution on SWCNT paper showed 90°, whereas the electrolyte with PEG-600 and HCHO delivered high wettability (55°). It was found that HCHO

is not involved in the wettability but is oxidized to formic, in which resulting electron is consumed by the reduction of  $\text{Sn}^{2+}$ . This is supported by the large amount of Sn particles obtained when co-addition of HCHO and PEG-600 (Figure 3d). It was reported that PEG adsorbs as a monolayer on the surface to inhibit electrodeposition reactions under the presence of  $\text{Cl}^-$ .<sup>10</sup> In fact, the reductive potential of  $\text{Sn}^{2+}$  shifted to the negative side at the addition of PEG into electroplating bath, meaning the delay of Sn electrodeposition reaction on SWCNT paper, as depicted in the cathodic polarization behavior (Figure 4b). We therefore considered that the synergetic effect generated from the enhanced wettability and the function as an inhibitory agent to excessive electrodeposition reaction on SWCNT surface permitted Sn nucleus to form inside the structure. The flexibility of the SWCNT/Sn composite paper was not detracted after electrodeposition, and the deposit did not peel off from the paper even when bent, suggesting high adhesiveness between SWCNT and Sn.

#### 4. Summary

The influence of HCHO and PEG on Sn electrodeposition behavior on SWCNT paper was studied. The co-addition of HCHO and PEG achieved the electrochemical preparation of SWCNT/Sn composite in which Sn is uniformly dispersed inside the SWCNT, by the respective effects of electron generation and good wettability.

#### Acknowledgments

This work was supported by a Grant-in-Aid for Research Activity Start-up (16H06838) from JSPS and a research grant from the Murata Science Foundation. The authors gratefully acknowledge Mr. S. Fujiwara, Mr. A. Sakai, and Dr. T. Yamagishi for their stimulating discussions and heartfelt advices.

#### References

1. S. Cao, X. Feng, Y. Song, X. Xue, H. Liu, M. Miao, J. Fang and L. Shi, *ACS Appl. Mater. Interfaces*, **7**, 10695 (2015).
2. S. Arai, K. Kirihata, M. Shimizu, M. Ueda, A. Katada and M. Uejima, *J. Electrochem. Soc.*, **164**, D922 (2017).

3. V. Mani, B. Devadas and S. M. Chen, *Biosens Bioelectron*, **41**, 309 (2013).
4. C. Subramaniam, T. Yamada, K. Kobashi, A. Sekiguchi, D. N. Futaba, M. Yumura and K. Hata, *Nat. Commun.*, **4**, 2202 (2013).
5. K. Hasegawa and S. Noda, *J. Power Sources*, **321**, 155 (2016).
6. M. Shimizu, R. Yatsuzuka, M. Horita, T. Yamamoto and S. Arai, *J. Phys. Chem. C*, **121**, 27285 (2017).
7. 17. Z. Yuan, H.-J. Peng, J.-Q. Huang, X.-Y. Liu, D.-W. Wang, X.-B. Cheng and Q. Zhang, *Adv. Funct. Mater.*, **24**, 6105 (2014).
8. K. Hata, D.N. Futaba, K. Mizuno, T. Namai, M. Yumura, S. Iijima, *Science*, **306**, 1362 (2004).
9. 21. J. S. Sharp, D. J. Farmer and J. Kelly, *Langmuir*, **27**, 9367 (2011).
10. J.J. Kelly and A.C. West, *J. Electrochem. Soc.*, **145**, 3472 (1998).

### Figure Captions

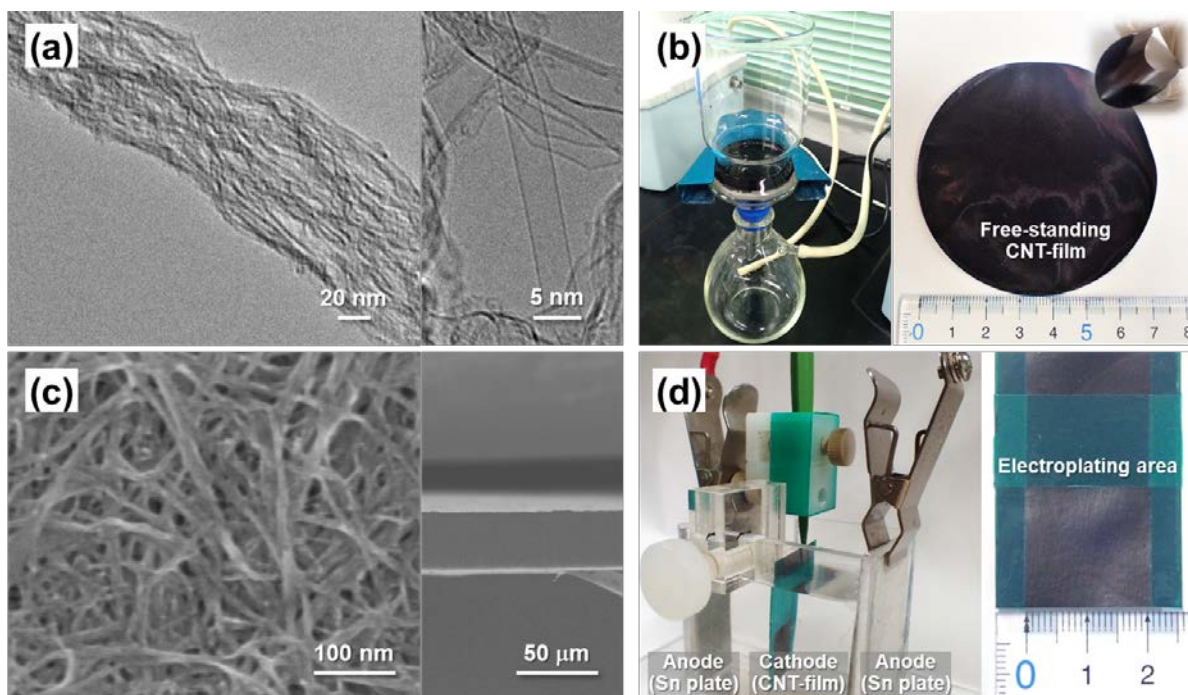
Figure 1 (a) HR-TEM images of SWCNTs. (b) Preparation scheme of a free-standing SWCNT paper by suction filtration from a suspension including SWCNT dispersed by SDBS. (c) Surface and cross-sectional FE-SEM images of the SWCNT paper. (d) Photograph during Sn electroplating.

Figure 2 (a) Raman spectra and XRD patterns of free-standing SWCNT films before and after Sn electroplating under the galvanostatic condition. Inset: Photographs of the SWCNT/Sn composites. For comparison, pristine SWCNT paper is also shown.

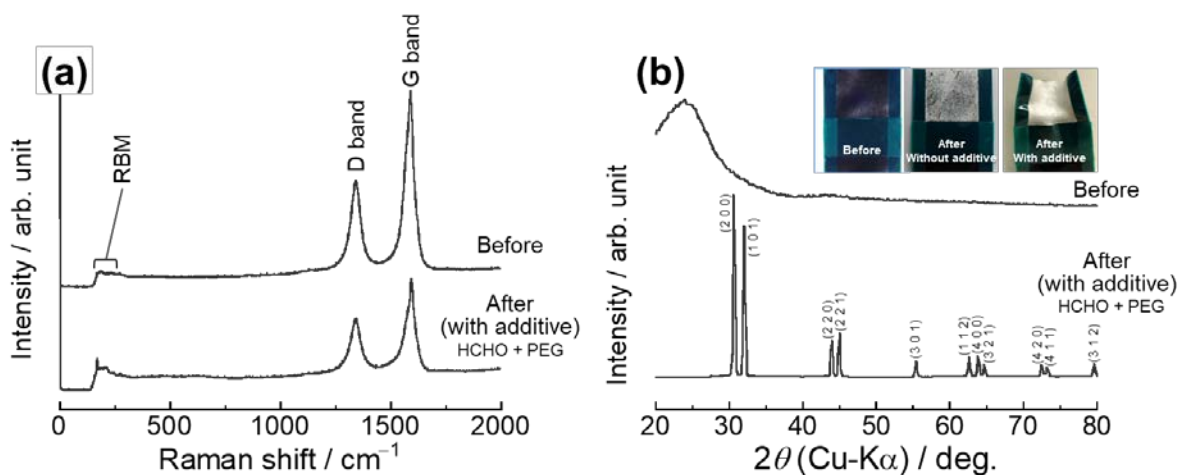
Figure 3 Cross-sectional FE-SEM images of SWCNT/Sn composites obtained from electroplating baths: (a) additive free (0.5 M SnCl<sub>2</sub> + 1.25 M K<sub>4</sub>P<sub>2</sub>O<sub>7</sub>), (b) with 5 mM HCHO, (c) with 2 mM PEG-600, (d) with 5 mM HCHO + 2 mM PEG-600.

Figure 4 (a) Droplets of aqueous-based electroplating baths (0.5 M SnCl<sub>2</sub> + 1.25 M K<sub>4</sub>P<sub>2</sub>O<sub>7</sub>) without and with additives. (b) Cathodic linear sweep voltammograms of Sn electrodeposition in the aqueous solutions. Inset: proposed mechanism of Sn electrodeposition inside SWCNT

paper in the electroplating bath with additives.



**Figure 1** (a) HR-TEM images of SWCNTs. (b) Preparation scheme of a free-standing SWCNT paper by suction filtration from a suspension including SWCNT dispersed by SDBS. (c) Surface and cross-sectional FE-SEM images of the SWCNT paper. (d) Photograph during Sn electroplating.



**Figure 2** (a) Raman spectra and XRD patterns of free-standing SWCNT films before and after Sn electroplating under the galvanostatic condition. Inset: Photographs of the SWCNT/Sn composites. For comparison, pristine SWCNT paper is also shown.

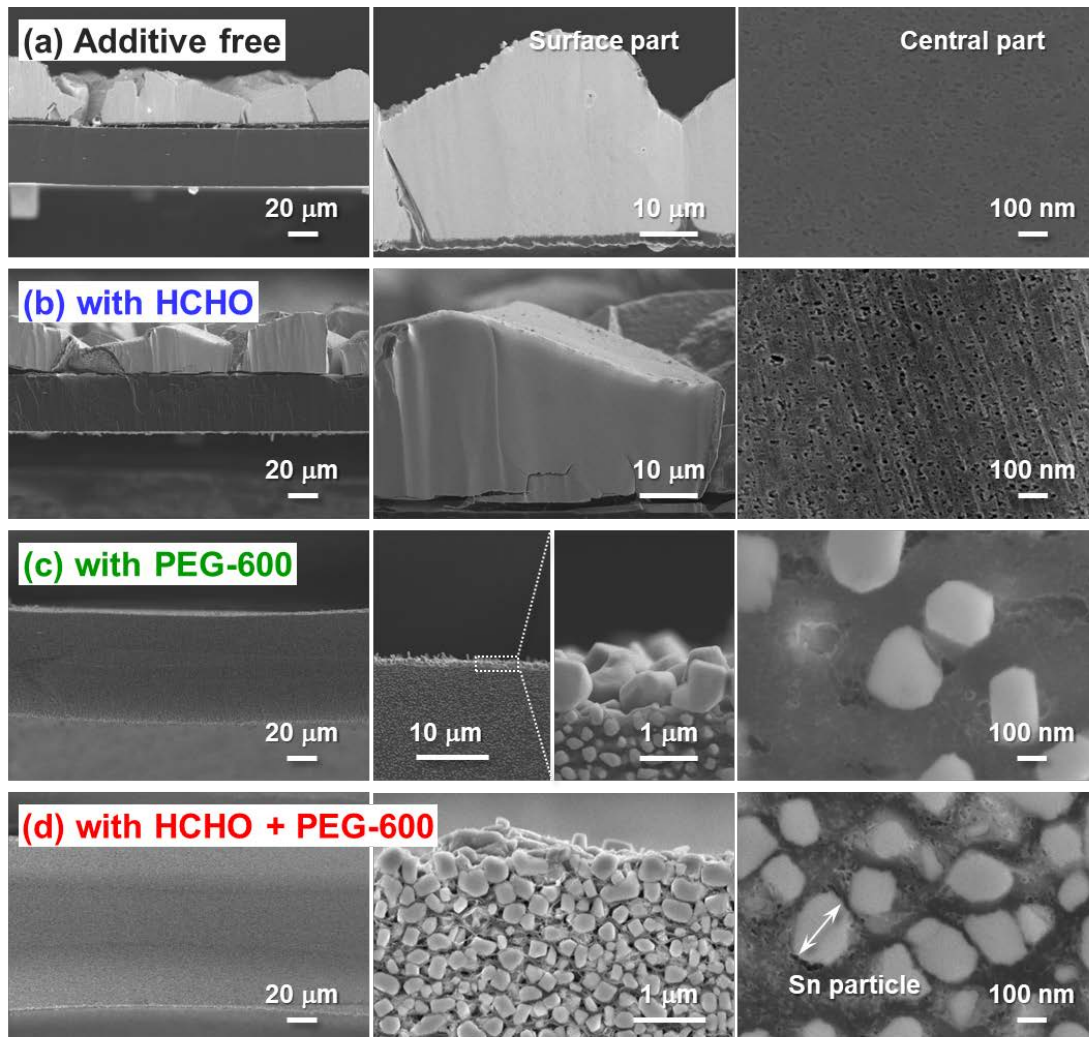


**Figure 3** Cross-sectional FE-SEM images of SWCNT/Sn composites obtained from electroplating baths: (a) additive free ( $0.5 \text{ M SnCl}_2 + 1.25 \text{ M K}_4\text{P}_2\text{O}_7$ ), (b) with  $5 \text{ mM HCHO}$ , (c) with  $2 \text{ mM PEG-600}$ , (d) with  $5 \text{ mM HCHO} + 2 \text{ mM PEG-600}$ .